

# Green synthesis of dihydroxybenzene from phenol with hydrogen peroxide catalyzed by iron modified FSM-16

Guanhua Luo<sup>1</sup> · Yujuan Jiao<sup>1</sup> · Xuechuan Lv<sup>1</sup> · Xiaofan Zhang<sup>1</sup> · Xiaohan Gao<sup>1</sup>

Received: 3 January 2018 / Accepted: 2 April 2018  
© Springer Science+Business Media B.V., part of Springer Nature 2018

**Abstract** Catechol and hydroquinone are very important fine chemical intermediate products, which have a wide range of applications. The hydroxylation of phenol with hydrogen peroxide to produce dihydroxybenzene is a mild and environmental friendly route. In this work, FSM-16 modified by iron (Fe/FSM-16) is used as a catalyst. With Fe content of 5% (wt), phenol to H<sub>2</sub>O<sub>2</sub> ratio of 3:1, reaction temperature of 60 °C, catalyst amount of 0.1 g and reaction time of 6 h, phenol conversion of 29.1% and dihydroxybenzene selectivity (catechol/hydroquinone = 1.6) of 93.5% are achieved. The results are close to that of TS-1 which is used in industry production and shows good prospects for industrial applications. The characterizations revealed that the Fe/FSM-16 could be reusable and stable.

**Keywords** Catalysis · Hydroxylation · Zeolites · Iron

## Introduction

The hydroxylation of phenol to dihydroxybenzene is a very important industrial process. The products, catechol and hydroquinone, are important fine manufactures used in many diverse fields. Catechol is widely used as a starting material for pharmaceutical, pesticide, perfume, dope and many fine chemicals. Hydroquinone is mainly used in photographic chemicals, antioxidants, flavoring agents, polymerization and inhibitors. Hydrogen peroxide has been regarded as a clean oxidant which afforded water as by-product [1]. Phenol oxidation with hydrogen peroxide to

---

✉ Xiaohan Gao  
gaoxhan@163.com

<sup>1</sup> School of Chemistry and Material Science, College of Chemistry, Chemical Engineering and Environmental Engineering, Liaoning Shihua University, Fushun 113001, Liaoning, China

dihydroxybenzene is considered as a promising and valuable chemical industrial process. The typical industrial processes to synthesize dihydroxybenzenes from phenol and hydrogen peroxide were catalyzed by inorganic acid or a molecular sieve, such as the Rhone-Poulenc process [2], using sulfuric acid as catalyst. The Enichem process [3] is now industrialized with high hydroquinone selectivity (hydroquinone/catechol ratio = 1) and high hydrogen peroxide efficiency, using TS-1 (titanium silicalite-1) as catalyst. Phenol conversion is 25%, and 90% of dihydroxybenzene selectivity is obtained. However, this process has many problems with separation, catalyst reclamation and expensive spending.

The catalysts with cheaper price, better performance, higher conversion and selectivity, easy recycle and simple preparation are the main direction of research. Many papers and monographs [4–6] concerning the process of hydroxylation of phenol to dihydroxybenzene, and the investigations concerning the catalyst for the process have been reported. The reported catalysts include complex metals oxide [7–9], modified molecular sieves [10–12], or heteropoly acid [13].

The family of silica-based mesoporous silica materials designated as M41S [14] has received considerable interest over the last years. They have some attractive characteristics, such as very high surface areas, regular mesopores and hydrophobicity. One of them, FSM-16 [15] (Folded-Sheet Mesoporous Material) is easily synthesized from a layered sodium silicate by using cetyltrimethylammonium cations as a template, and the raw material is cheaper and convenient to obtain.

In this work, the FSM-16 was selected as the carrier and modified by iron. Effects of the Fe capacity, the ratio of phenol to hydrogen peroxide, temperature and catalyst dosage on the catalytic performances for hydroxylation of phenol to catechol and hydroquinone were investigated. Catalysts were characterized with X-ray diffraction (XRD),  $\text{NH}_3$ -TPD and  $\text{N}_2$  adsorption–desorption experiment.

## Experimental

### Materials and reagents

All the above reagents were of analytical grade and obtained from the Sinopharm Chemical Reagent Co. Ltd.

### Catalyst preparation

FSM-16 was typically prepared by the following procedure as in the literature [16, 17], kanemite crystals (10.0 g) obtained by calcinations of a water glass ( $\text{SiO}_2/\text{Na}_2\text{O} = 2$ ) at 500 °C for 5 h were dispersed in 100 mL water and stirred for 3 h at room temperature. After filtration, the wet kanemite was dispersed in cetyltrimethylammonium bromine aqueous solution (200 mL 0.1 mol/L) with stirring for 3 h at 70 °C. The pH of the suspension was adjusted to 8–9 by addition of 2 mol/L HCl solution again and the suspension was left at 70 °C for a further 3 h. After filtration, the sample was dried at 120 °C and calcined at 500 °C for 5 h to remove the surfactant to obtain FSM-16.

FSM-16 modified by iron was typically prepared by the following procedure, Iron(III) nitrate nonahydrate was dissolved in 20 mL of water and then FSM-16 (5.0 g) was added in the solution. The above slurry was stirred and dried at room temperature. Finally, the product was calcined at 500 °C for 5 h and Fe/FSM-16 was obtained.

## Hydroxylation reaction and products analysis

The hydroxylation of phenol with hydrogen peroxide was carried out in a 100 mL flask with thermometer and condensator. In the typical run, 0.1 g of catalyst, 0.02 mol of phenol and 20 mL of water were placed in the reactor and heated. Hydrogen peroxide (30%) was added dropwise through a dropping funnel. The addition rate was controlled at 0.1 mL per min. After the complete addition of hydrogen peroxide, the mixture was further stirred at a certain temperature for 6 h and then cooled down to room temperature. The GC analyses (GC-7900, *Shanghai Techcomp Instrumengts Ltd*) of products were performed with an OV-1 capillary column (35 m × 0.32 mm × 0.8 μm) using benzyl alcohol as an internal standard.

## Characterization of catalysts

Powder X-ray diffraction (XRD) patterns were recorded using Rigaku D/Max 3400 X (Rigaku Corporation Jan) with Cu K $\alpha$  radiation at 0.02 steps per second in angle range  $2\theta = 5^\circ\text{--}90^\circ$ .

Low-temperature N<sub>2</sub> adsorption–desorption experiments were carried out using a Quantachrome Autosorb-1 system (*Quantachrome Instruments U.S.*). The modal pore diameter was calculated using the BJH method based on the desorption isotherm, and the surface area was calculated using the BET method based on the adsorption isotherm.

NH<sub>3</sub>-TPD (temperature-programmed desorption) experiments were performed using AutoChem II 2920 (*Micromeritics Instrument Corporation U.S.*). Before the adsorption of NH<sub>3</sub>, the sample (~ 0.1 g) was pretreated at 350 °C in He (30 mL/min) for 30 min. Then the sample was cooled down to 100 °C and adsorbed NH<sub>3</sub> for 0.5 min. Subsequently, the catalyst was flushed with He until the baseline was steady. The desorption process was monitored with a thermal conductivity detector at a temperature ramp from 100 to 500 °C, with a heating rate of 15 °C/min.

## Results and discussion

### Effect of the Fe content

The results of hydroxylation of phenol over mesoporous silica materials FSM-16 modified by different Fe content are shown in Table 1. Phenol conversion of 2.8% is obtained over the unmodified FSM-16. The product is only benzoquinone. As Fe(NO<sub>3</sub>)<sub>3</sub>·9H<sub>2</sub>O was used as catalyst alone, the conversion of phenol is 23.5%, and

**Table 1** Effect of Fe contents in catalysts

Content of Fe/ wt%	Phenol conversion/%	Products distribution/%			Catechol/ hydroquinone/mol
		Catechol	Hydroquinone	Benzoquinone	
FSM-16	2.8	0	0	100	–
Fe/FSM-16 (0.5)	18.9	30.2	0	69.8	–
Fe/FSM-16 (1.5)	18.1	50.3	24.3	25.4	2.1
Fe/FSM-16 (2.5)	22.1	50.9	29.9	19.2	1.7
Fe/FSM-16 (5.0)	27.5	55.5	31.9	12.6	1.7
Fe/FSM-16 (7.5)	26.3	52.9	32.8	14.3	1.6
Fe/FSM-16 (10.0)	27.4	53.1	33.6	13.3	1.6
Fe(NO <sub>3</sub> ) <sub>3</sub> ·9H <sub>2</sub> O	23.5	54.1	27.8	18.1	1.9

Reaction condition:  $n(\text{phenol}):n(\text{H}_2\text{O}_2) = 3:1$ , catalyst 0.1 g, temperature 50 °C, time 6 h

the selectivity of dihydroxybenzene is 81.9%. However, it is homogeneous catalytic reaction and Fe(NO<sub>3</sub>)<sub>3</sub>·9H<sub>2</sub>O is impossible to be reused.

Phenol conversion and dihydroxybenzene selectivity increased obviously at the presence of the FSM-16 modified by iron (Fe/FSM-16) in the reaction that illuminates Fe is the active center of the Fe/FSM-16. The formation of benzoquinone is restrained over Fe/FSM-16. It can be seen from the performances of catalysts with different Fe content that the conversion of phenol increased as the Fe content increased. The catalyst with Fe content of 5.0% (wt) displays the highest phenol conversion of 27.5% and dihydroxybenzene selectivity of 87.4%. The ratio of catechol to hydroquinone is 1.6 that is in accord with the industrial desirability. When Fe content is more than 5.0% (wt), the conversion of phenol has little change. The low Fe content causes the less active center, which is not a benefit to the activation of H<sub>2</sub>O<sub>2</sub>. Then the conversion of phenol is low. Small amounts of generated hydroquinone are easily oxidized to benzoquinone that result in the low hydroquinone selectivity. The active center increased as the Fe content increased. Then phenol conversion increased, the amount of generated hydroquinone increased and hydroquinone selectivity increased. However, the catalyst activity center increased slightly when Fe content is more than 5.0% (wt). Phenol conversion and dihydroxybenzene selectivity remained. Therefore, the optimum Fe content was 5.0% (wt).

### Effect of the ratio of phenol to hydrogen peroxide

Effect of the ratio of phenol to hydrogen peroxide in the reaction is shown in Table 2. Conversion of phenol increased a little as the hydrogen peroxide dosage

**Table 2** Effect of the ratio of phenol to hydrogen peroxide

Phenol/ H <sub>2</sub> O <sub>2</sub> /mol	Phenol conversion/ %	H <sub>2</sub> O <sub>2</sub> utilization/ %	Products distribution/%		
			Catechol	Hydroquinone	Benzoquinone
3:1	27.5	82.5	55.5	31.9	12.6
3:2	30.4	44.5	49.8	26.5	23.7
3:3	39.1	39.1	48.0	25.9	26.1

Reaction condition: Fe content 5.0% (wt), catalyst 0.1 g, temperature 50 °C, time 6 h

increased. However, the utilization of hydrogen peroxide and the selectivity of dihydroxybenzene decreased sharply. The decomposition rate of hydrogen peroxide to O<sub>2</sub> and OH<sup>-</sup> increased as the concentration of hydrogen peroxide increased [18]. The higher decomposition rate of hydrogen peroxide lead to the higher concentration of OH<sup>-</sup> that easily oxidized hydroquinone to benzoquinone. As a result, the utilization of hydrogen peroxide and the selectivity of dihydroxybenzene decreased. It is found that the quick addition speed of hydrogen peroxide results in the decrease of the dihydroxybenzene selectivity during the experiments. From the point of the economic efficiency, the optimum ratio of phenol to hydrogen peroxide is 3:1, and the addition speed of hydrogen peroxide must be slow.

### Effect of the reaction temperature

Table 3 is the influence of reaction temperature on the catalytic performance in the reaction. Fe/FSM-16 exhibits high catalytic activity for hydroxylation of phenol with hydrogen peroxide to produce dihydroxybenzene at low temperature. Conversion of phenol increased firstly and then decreased with increasing the reaction temperature. Excellent phenol conversion of 29.1% with dihydroxybenzene selectivity of 93.5% was obtained at 60 °C. Catalyst had lower efficiency to activate hydrogen peroxide which accounts for the lower phenol conversion at low temperature. The decomposition rate of hydrogen peroxide to O<sub>2</sub> and OH<sup>-</sup> increased

**Table 3** Effect of reaction temperature

Temperature/°C	Phenol conversion/%	Products distribution/%		
		Catechol	Hydroquinone	Benzoquinone
30	18.2	55.5	26.4	18.1
40	21.1	50.1	23.5	24.3
50	27.5	55.5	31.9	12.6
60	29.1	55.6	37.9	6.5
70	26.9	50.2	28.3	21.5
80	20.9	46.3	32.3	21.4

Reaction condition:  $n(\text{phenol}):n(\text{H}_2\text{O}_2) = 3:1$ , catalyst 0.1 g, Fe content 5.0% (wt), time 6 h

at higher temperature that lead to the utilization of hydrogen peroxide decreasing. More amounts of generated OH<sup>-</sup> oxidized hydroquinone to benzoquinone that decreased the selectivity of dihydroxybenzene. From the energy saving and yield of dihydroxybenzene point of view, the optimum temperature for the reaction is between 50 and 60 °C.

### Performance of recycling Fe/FSM-16 (5.0 wt%)

The used Fe/FSM-16 (5.0 wt%) catalyst was separated by filtration, washed with copious amounts of water and calcined at 500 °C for 5 h. Table 4 is the reusability test results of the Fe/FSM-16 (5.0 wt%) catalyst. The activity of Fe/FSM-16 (5.0 wt%) catalyst changed a little so that phenol conversion is about 29.0% from first run to third run. In the fourth run, the conversion of phenol dropped to 26.1%. The selectivity of dihydroxybenzene decreased at the second run and remained stable from the second run to fourth run. The reason may be that some of the active centers of the catalyst may be leached out or become inactive. The recycling test confirms that the catalyst is reusable.

### XRD analysis of FSM-16 and Fe/FSM-16 (5.0 wt%)

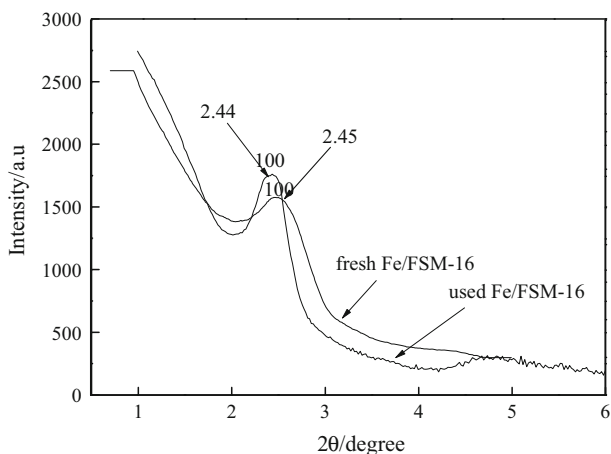
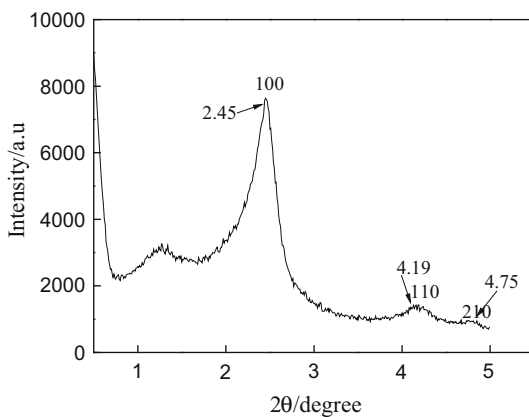
A powder low angle XRD pattern of FSM-16 is shown in Fig. 1. The curve of FSM-16 showed the typical diffraction patterns of silica-based mesoporous molecular sieves in the low-angle region [19]. Three peaks of (100) (110) and (210) appear at 2.45°, 4.19° and 4.75°. The corresponding d values of FSM-16 are 3.55, 1.90 and 1.67 nm calculated by the formula  $2d\sin\theta = \lambda$ .

Figure 2 is the powder low angle XRD patterns of fresh Fe/FSM-16 (5.0 wt%) and used Fe/FSM-16 (5.0 wt%). A widened peak of  $d_{100}$  is observed in the curve of Fe/FSM-16. However, the  $d_{100}$  peak location does not shift ( $2\theta = 2.45^\circ$ ). The peaks of  $d_{110}$  and  $d_{210}$  disappear in the curve of Fe/FSM-16. Because of the support action of iron oxide and the interaction between iron oxide and the framework of FSM-16, some of the {100} planes were covered and regularity of the {100} planes was disturbed. Therefore, the diffraction intensity of the {100} planes weakened. The peaks of  $d_{110}$  and  $d_{210}$  are too weak to appear.

**Table 4** Performance of recycling Fe/FSM-16 (5.0 wt%)

Recycle time	Phenol conversion/%	Products distrobution/%		
		Catechol	Hydroquinone	Benzoquinone
1	29.1	55.6	37.9	6.5
2	28.5	52.1	33.5	14.4
3	28.7	54.5	32.9	12.6
4	26.1	53.6	32.3	13.1
5	25.8	52.3	38.3	12.4

Reaction condition:  $n(\text{phenol}):n(\text{H}_2\text{O}_2) = 3:1$ , catalyst 0.1 g, Fe content 5.0% (wt), time 6 h

**Fig. 1** XRD pattern of FSM-16 (5.0 wt%)**Fig. 2** XRD patterns of fresh Fe/FSM-16 (5.0 wt%) and used Fe/FSM-16 (5.0 wt%)

The powder low angle XRD pattern of the used Fe/FSM-16 (5.0 wt%) is similar to that of the fresh Fe/FSM-16 (5.0 wt%). It shows that the used Fe/FSM-16 had no obvious change compared with the fresh Fe/FSM-16 and the catalyst structure and crystallinity were stable.

### NH<sub>3</sub>-TPD of catalysts

It is known that the acid sites of molecular sieves are related to their catalytic oxidation activity. Therefore, it is essential to analyze the acidity of the catalyst in detail. The acid strength of the zeolites was analyzed by NH<sub>3</sub>-TPD (Fig. 3). The strength distribution of the acid sites is estimated from the deconvolution of the TPD plots with Gaussian curves [20]. The results are listed in Table 5. Fe content of FSM-16 is connected with the surface acidity and hydrophobicity of catalyst [21]

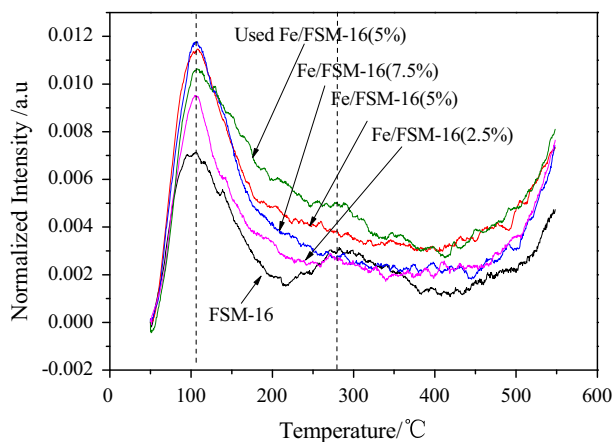


**Fig. 3**  $\text{NH}_3$ -TPD profiles of catalysts

**Table 5** Acidity of catalysts

Catalysts	Total acid sites <sup>a</sup> (mmol/g)	Weak acid sites <sup>b</sup> (mmol/g)	Strong acid sites (mmol/g)
FSM-16	0.295	0.242	0.053
Fe/FSM-16 (2.5%)	0.401	0.401	–
Fe/FSM-16 (5.0%)	0.533	0.533	–
Fe/FSM-16 (7.5%)	0.438	0.438	–
Fe/FSM-16 (5%)	0.565	0.565	–

<sup>a</sup>Determined by  $\text{NH}_3$ -TPD

<sup>b</sup>The peak centered below 280 °C was defined as  $\text{NH}_3$  desorbed from weak acid sites

that is related to the catalytic performance. Two desorption peaks that appeared at 107 and 294 °C in the curve of FSM-16 are assigned to the weak and medium acid sites, respectively. The peak assigned to the weak acid sites still appeared at 107 °C in the curve of Fe/FSM-16, and the weak acid sites increased obviously as the Fe content increased (0, 2.5, 5.0%). It illuminating that the amount of weak acid sites great increased, and acid strength had no change. Then, the catalyst activity increased. The weak acid sites of the Fe/FSM-16 (7.5 wt%) are less than that of the Fe/FSM-16 (5.0 wt%) (Table 5) whereas the catalyst activity of the Fe/FSM-16 (7.5 wt%) is close to that of the Fe/FSM-16 (5.0 wt%) (Table 1). It indicates that the effect of the amount of weak acid sites on catalyst activity is not significant when the weak acid sites amount exceeds a certain level.

The weak acid sites of the used Fe/FSM-16 (5.0 wt%) are more than that of the fresh Fe/FSM-16 (5.0 wt%). It can be seen from Fig. 3 that the acid strength had a little addition which caused the increase of benzoquinone selectivity (Table 4). However, the peak at 294 °C assigned to the medium acid disappeared in the curve

of Fe/FSM-16. It is concluded from the result of  $\text{NH}_3$ -TPD and effects of the Fe content on the catalytic performance (Table 1) that weak acid sites were at the catalyst active center which is responsible for the hydroxylation of phenol with hydrogen peroxide to produce catechol and hydroquinone. The conversion of phenol increased and reached the best result as the Fe content increased that is accordant with the variation trend of weak acid sites with the Fe content addition.

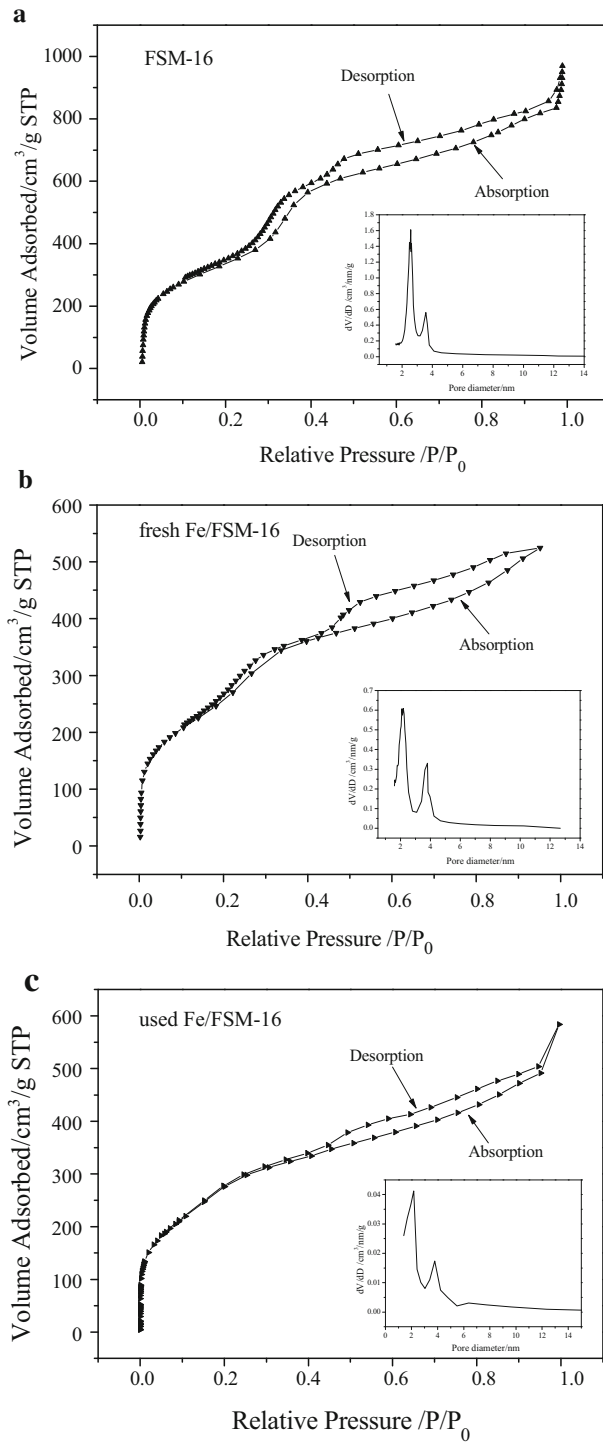
### **$\text{N}_2$ adsorption–desorption isotherms of FSM-16, fresh and used Fe/FSM-16 (5.0 wt%)**

$\text{N}_2$  adsorption–desorption isotherms and pore distribution profiles of FSM-16, fresh Fe/FSM-16 (5.0 wt%) and used Fe/FSM-16 (5.0 wt%) are given in Fig. 4. The FSM-16 sample (Fig. 4a) exhibited type IV isotherms (defined by IUPAC) with a small hysteresis loop [22], which is characteristic for the capillary condensation in the mesopores. The initial part of the isotherm (until  $p/p^\circ \approx 0.2$ ) can be attributed to monolayer-multilayer adsorption because it follows the same path of desorption, which demonstrates weak adsorbate-adsorbent interactions. The hysteresis loop is of type H3, which is usually indicative of aggregates of platelet particles or adsorbents containing slit pores. Figure 4b, c clearly shows that less nitrogen was adsorbed on fresh Fe/FSM-16 (5.0 wt%) and used Fe/FSM-16 (5.0 wt%) than on FSM-16. This finding can be attributed to the pore blocking by iron oxide particles which is dispersed on the inner wall of pore. The IUPAC classifies the adsorption curves as type IV and the hysteresis loop types as H3, which is similar to the FSM-16 case.

The nitrogen sorption study showed that the BET surface area of FSM-16 is  $1318 \text{ m}^2 \text{ g}^{-1}$  and the mesopore volume is  $1.59 \text{ cm}^3 \text{ g}^{-1}$ . The average pore diameter is calculated to be 2.94 nm using the BJH method. For Fe/FSM-16 (5.0 wt%), the BET surface area is  $993 \text{ m}^2 \text{ g}^{-1}$  and the mesopore volume is  $0.88 \text{ cm}^3 \text{ g}^{-1}$ . The average pore diameter is 2.69 nm. The change is due to that the iron oxide particles blocking the macropores and some larger mesopores, leaving the smaller mesopores for the reactants. The pore size distribution of Fe/FSM-16 (5.0 wt%) shrinks compared to that of FSM-16. It indicates that the iron oxide particles were dispersed on the inner wall of pores. In the case of used Fe/FSM-16 (5.0 wt%), the BET surface area is  $996 \text{ m}^2 \text{ g}^{-1}$  and the mesopore volume is  $0.94 \text{ cm}^3 \text{ g}^{-1}$ . The average pore diameter is 2.60 nm. The results were similar to that of the fresh Fe/FSM-16 (5.0 wt%).

## **Conclusions**

In summary, Fe/FSM-16 is shown to be an efficient catalyst for the hydroxylation of phenol to catechol and hydroquinone. Phenol conversion and dihydroxybenzene selectivity increased greatly after the FSM-16 was modified by iron. The optimized reaction conditions are that the dosage of catalyst is 0.1 g, Fe content is 5.0% (wt), temperature is  $60^\circ \text{C}$ , reaction time is 6 h and  $n(\text{phenol}):n(\text{H}_2\text{O}_2) = 3:1$ . Phenol conversion of 29.1% and dihydroxybenzene selectivity (catechol/hydroquinone = 1.6) of 93.5% were achieved. The catalytic performance of Fe/FSM-16



◀ **Fig. 4** N<sub>2</sub> absorption–desorption isotherms and pore distribution profiles for FSM-16 (a), fresh (b) and used (c) Fe/FSM-16 (5.0 wt%)

is close to that of TS-1 used in industry production. Moreover, Fe/FSM-16 is characterized with simple short-period preparation, abundant availability for the raw material and relatively cheap cost. All of these show excellent prospects for industrial applications. The results of NH<sub>3</sub>-TPD show that the weak acid sites are an active center and responsible for the catalytic activity. The amount of weak acid sites increased as the Fe content increased. The catalytic activity reached the maximum. The research of the catalyst N<sub>2</sub> absorption–desorption isotherms illustrates that the iron oxide particles were dispersed on the inner wall of pores and blocked the macropores and some larger mesopores, leaving the smaller mesopores to benefit from the reaction. The used catalyst structure, crystallinity, acid density, surface area, mesopore volume and pore diameter changed a little. It showed that the Fe/FSM-16 is stable and reusable.

**Acknowledgements** The work was financially supported by the National Nature Science Foundation of China under the grant NSFC. Nos. 21103078, 21003069.

## References

1. T. Atoguchi, T. Kanougi, *J. Mol. Catal. A Chem.* **222**, 253 (2004)
2. A. Thangaraj, R. Kumar, P. Ratnanasmy, *J. Catal.* **131**, 294 (1991)
3. X.B. Ma, S.P. Wang, J.L. Gong, X. Yang, G.H. Xu, *J. Mol. Catal. A Chem.* **222**, 183 (2004)
4. L. Hai, T.Y. Zhang, X. Zhang, G.H. Zhang, B. Li, S. Jiang, X.Y. Ma, *Catal. Commun.* **101**, 93 (2017)
5. Y. Shao, H.H. Chen, *Chem. Eng. Res. Des.* **132**, 57 (2018)
6. N. Inchaurredo, C.P. Ramos, G. Žerjav, J. Font, A. Pintar, P. Haure, *Micropor. Mesopor. Mater.* **239**, 396 (2017)
7. S. Pithakratanayothin, R. Tongstri, T. Chaisuwan, S. Wongkasemjit, *Mater. Chem. Phys.* **181**, 452 (2016)
8. W.J. Zhang, Y.Z. Wang, Y. Shen, M.J. Xie, X.F. Guo, *Micropor. Mesopor. Mater.* **226**, 278 (2016)
9. O. Amadine, Y. Essamlali, A. Fihri, M. Larzek, M. Zahouily, *RSC Adv.* **7**, 12586 (2017)
10. A. Kessouri, B. Boukoussa, A. Bengueddach, R. Hammcha, *Res. Chem. Intermed.* **44**, 2475 (2018)
11. G.Q. Wu, J.H. Xiao, L. Zhang, W.J. Wang, Y.P. Hong, H.J. Huang, Y. Jiang, L. Li, C.R. Wang, *RSC Adv.* **6**, 101071 (2016)
12. D.X.M. Vargas, J.R.D.L. Rosa, S.A. Iyoob, C.J. Lucio-Ortiz, F.J.C. Córdoba, C.D. Garcia, *Appl. Catal. A Gen.* **506**, 44 (2015)
13. K. Pamin, J. Połtowicz, M. Prończuk, S. Basąg, J. Maciejewska, J. Kryściak-Czerwenk, R. Tokarz-Sobieraj, *Catal. Today* **257**, 80 (2015)
14. C.T. Kresge, M.E. Leonowicz, W.J. Roth, J.C. Vartuli, J.S. Back, *Nature* **359**, 710 (1992)
15. O. Jkdetchai, N. Takayama, T. Nakajima, *Kinet. Catal.* **46**, 56 (2005)
16. S. Inagaki, Y. Fukushima, K. Kurodab, *J. Chem. Soc. Chem. Commun.* **46**, 680 (1993)
17. T. Yamamoto, T. Tanaka, T. Funabiki, *J. Phys. Chem. B* **102**, 5830 (1998)
18. D.R.C. Huybrechts, P.L. Buskens, P.A. Jacobs, *J. Mol. Catal.* **71**, 129 (1992)
19. B.J. Aronson, C.F. Blanford, A. Stein, *Chem. Mater.* **9**, 2842 (1997)
20. L.P. Zhou, Z. Liu, Y.Q. Bai, T.L. Lu, X.M. Yang, J. Xu, *J. Energy Chem.* **25**, 141 (2016)
21. M.M. Mohameda, N.A. Eissab, *Mater. Res. Bull.* **38**, 1993 (2003)
22. W.Q. Pang, J.H. Yu, Q.S. Huo, J.S. Chen, in *Zeolite and Porous Material Chemistry*, ed. by R.R. Xu (Science Press, Beijing, 2004), p. 146